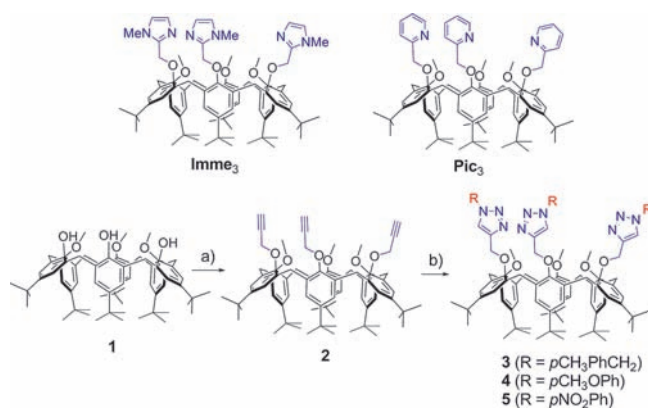


Scheme 1. (Bottom) Synthesis of the Triazolyl Ligands^{a,b} and (Top) Representation of the Imme₃ and Pic₃ Related Ligands



^a Propargylbromide, Cs₂CO₃, DMF, 150 °C, 93%. ^b RN₃, CuSO₄·5H₂O, Na ascorbate, CH₂Cl₂/H₂O, RT, ca. 75%.

the frame of a protein backbone. It also maintains a free coordination site in a well-controlled environment accessible via the cavity.^{10,11} Indeed, we have extensively studied the metal complexes based on the **Imme**₃ tripod ligand and found that their biomimetic properties do not only depend on the first coordination sphere. The second coordination sphere provided by the oxygen-rich small rim of the calixarene also plays a decisive role in the stabilization of a guest donor as well as the hydrophobic cavity acting as a funnel for the selective access of an exogenous ligand. Herein, we report the synthesis of three different tridentate tris(triazolyl) ligands and describe their coordination and host–guest properties with a hard dicationic metal ion, Zn(II), and with a soft monocationic one, Cu(I), together with some electrochemical features. A comparison with the structurally analogous tris(imidazolyl)- and tris(pyridyl)-calix[6]arene derivatives¹² (**Pic**₃, see Scheme 1) allows the highlighting of a number of interesting properties.

RESULTS

Synthesis of the Ligands. In order to obtain valuable data on the coordination behavior of tris(triazolyl) ligands based on calix[6]arenes, a key feature is the number of atoms separating the coordinating N-donor site and the phenoxy units to which they are attached. The best situation is when two atoms separate the N donors from the OAr units. Indeed, we have previously observed that a longer spacer brings too much flexibility and jeopardizes the coordination ability of the resulting ligand.¹³ The introduction of triazoles at the small rim of calix[6]arenes via the CuAAC procedure can be envisioned in two ways: an azido-calixarene reacting with alkynes or an alkyne-substituted calixarene reacting with organic azides. A calixarene building block for the first approach was recently reported.¹⁴ However, preliminary experiments done in collaboration with Jabin et al. for the coordination of Zn(II) cation were unsuccessful,¹³ suggesting that the triazolyl-calixarene derivatives presenting a three-atom spacer instead of a two-atom spacer are not optimal for the formation of the complex. In order to geometrically stick as much as possible to the parent **Imme**₃ and **Pic**₃ ligands extensively studied in our laboratory, we decided to use the alternative strategy. We first introduced the alkyne groups on trimethoxycalixarene **1** via alkylation of the phenol rings (Scheme 1).¹⁵

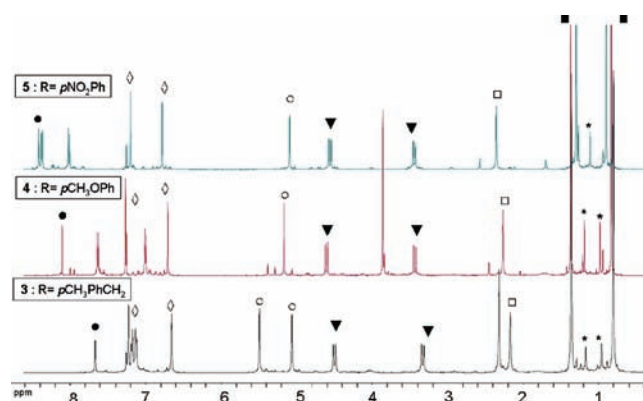
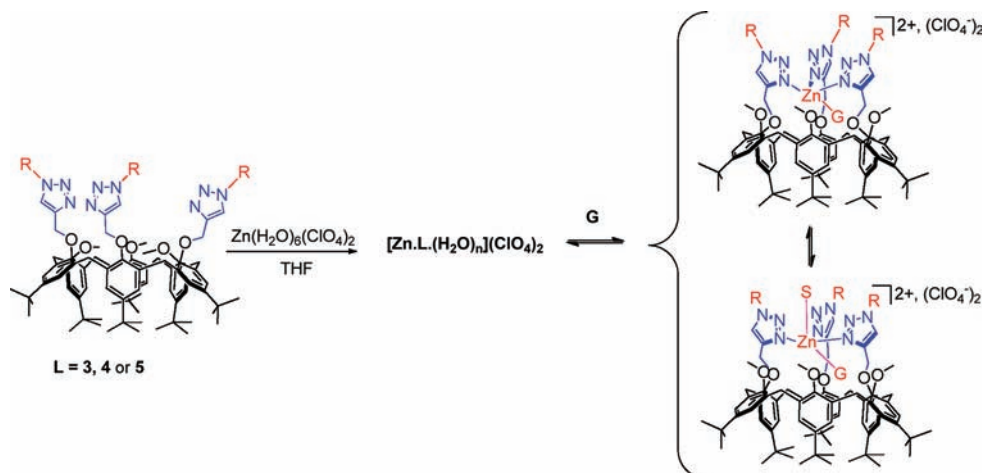


Figure 1. ¹H NMR (CDCl₃, 500 MHz, 300 K) spectra of ligands **3**, **4**, and **5** (from bottom to top). (■) *t*Bu, (□) OCH₃, (▼) ArCH₂, (○) triaCH₂, (◇) H_{Ary}, (●) H_{tria} (* minor conformations).

This reaction was performed in DMF at 150 °C with an excess of propargylbromide and cesium carbonate. Tris(propargyl)-calixarene **2** was obtained in 93% yield. The versatility of the CuAAC procedure enabled us to synthesize three different triazolyl-calixarene ligands. The reaction was carried out in the biphasic solvent mixture CH₂Cl₂/H₂O at room temperature with copper sulfate reduced in situ by sodium ascorbate as a catalyst. Compounds **3**, **4**, and **5** were isolated in good yields (ca. 75%).

In each case, ESI-MS experiments indicated the clean reaction of all three acetylene groups with two peaks at *m/z* corresponding to the monoprotonated ligand and the sodium adduct (see the Supporting Information). No peak associated with products bearing only one or two triazoles was observed. ¹H NMR spectra of the three ligands in CDCl₃ are very similar and in good agreement with the C_{3v} symmetry of the molecules in a cone conformation (Figure 1). Two resonances at ca. 0.7 and 1.4 ppm associated with peaks at 6.6 and 7.2 ppm account for the *t*Bu-phenoxy units of the calixarene. The resonance for the methoxy groups is a singlet at 2.1–2.2 ppm, which indicates that all three methoxy groups point inside the cavity. These observations denote a flattened cone conformation with three aromatic units being oriented toward the inside of the cone of the calixarene, the three other ones being projected away from it. Finally, the resonances of the protons for the methylene bridges are split into two doublets at ca. 3.3 ppm and 4.5 ppm, in agreement with a slow cone–cone inversion. The small resonances that can be detected especially between the two *t*Bu peaks attest to the presence of minor conformers, as observed for other tridentate ligands of the same family.^{8c,12a} Indeed, variable temperature ¹H NMR experiments showed that these small peaks tend to vanish upon heating the solution. Interestingly, the chemical shift of the protons located on the triazole units, H_{tria}, appears to be an excellent reporter of the electron density on the triazolyl rings: the more electron-withdrawing the substituent (*p*NO₂Ph > *p*CH₃OPh > *p*CH₂PhCH₂), the higher field the resonance (8.4 > 8.2 > 7.8 ppm). Surprisingly, even some protons belonging to the calixarene macrocycle are affected by the nature of the R substituents, albeit located far away from the triazoles (H_{Ary}, ArCH₂, *t*Bu, and OCH₃). This shows that the substitution pattern has a remote effect on the conformation of the calixarene cores.

We then evaluated the impact that the difference in triazole electron density would have on the coordination properties of the ligands as well as on the host–guest properties of the corresponding Zn(II) and Cu(I) metal complexes.

Scheme 2. Synthesis of the Zinc Complexes in THF and Schematic Representation of the Host–Guest Complexes^a

^a R = *p*NO₂Ph, *p*CH₃OPh, or *p*CH₃PhCH₂; S = residual water or coordinating solvent; G = guest ligand = H₂O or MeCN or PrNH₂ (see text).

Zn(II) Complexes and Host–Guest Studies. The complexes were prepared by adding 1 equiv of Zn(H₂O)₆(ClO₄)₂ into a solution of ligand 3, 4, or 5 in THF (Scheme 2) and isolated by precipitation with pentane. In the case of ligand 3, the ¹H NMR spectrum in CDCl₃ at 300 K clearly indicates the formation of a well-defined Zn(II) complex (Figure 2). Although slightly broader compared to the free ligand, the resonances attest to a C_{3v} symmetrical compound. The important downfield shift (+0.8 ppm) observed for the triazolyl protons agrees with the coordination of Zn(II) to all three triazole groups. Other changes in chemical shifts related to the calixarene core are quite similar to those observed for the tris(imidazole) parent complex.⁸ For instance, the resonance for the methoxy protons belonging to the calixarene core is strongly shifted downfield (+ 1.2 ppm). This indicates a conformational switch during the complexation event. Indeed, the aromatic units of the calixarene must flip one relative to the other in order to allow all three triazoles to coordinate the zinc cation, thus moving the methoxy groups away from the cavity, as illustrated in Scheme 2. Finally, the peak of the residual water is much broader than in the case of the spectrum of the free ligand and shifted downfield by ca. 0.6 ppm. This shows that water interacts with the metal center and that the coordinated water molecule is in fast exchange with free water. In anhydrous CDCl₃, some resonances are sharper (H_{tria} for instance), proving the role of water in structuring the metal complex (see Figure S1 in Supporting Information). Finally, the dicationic nature of the Zn(II) complexes is confirmed by elemental analyses. All of this information accounts for the formation of a host–guest complex, as depicted in Scheme 2 with G = H₂O. At this point, we cannot discriminate between a four- or a five-coordinate species where residual water (S = H₂O) is also in interaction in the exo position with the metal center as has been previously observed with Imme₃ coordinated to other metal dications such as Cu(II),^{9b} Ni(II), and Co(II)¹⁶ (vide infra in the Discussion).

For ligand 4, the ¹H NMR spectrum of the product resulting from the addition of Zn(II) is clearly different from the spectrum of the ligand itself as well (Figure S3, Supporting Information). The new resonances of H_{tria} at δ = 9.03 ppm and of OCH₃ at δ = 3.21 ppm are in good agreement with the formation of the complex. However, when the spectrum was recorded at 265 K,

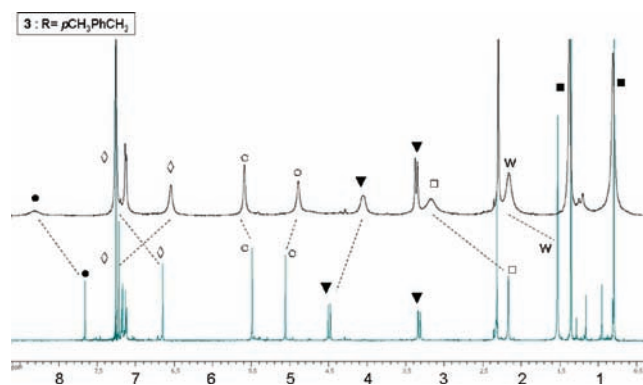


Figure 2. ¹H NMR (CDCl₃, 500 MHz, 300 K) spectra of ligand 3 (bottom) and complex [Zn·3·(H₂O)_n](ClO₄)₂ (top). (■) *t*Bu, (□) OCH₃, (▼) ArCH₂, (○) triaCH₂, (◇) ArH, (●) H_{tria} (w: residual water).

a number of new peaks denoting other conformations or species appeared (which stands in contrast with complex [Zn·3·(H₂O)_n](ClO₄)₂, see Figures S2 and S4, Supporting Information). This shows that, unlike in the case of ligand 3, the C_{3v} complex of 4 is not the only species present in solution. In the case of ligand 5, the presence of the Zn(II) did not even change the spectrum. Obviously, the ability of the calixarene-based ligands to complex the zinc cation depends on the coordination properties of the nitrogen arms. It has already been reported that the substitution of 1,4-disubstituted-1,2,3-triazoles can finely tune their coordination ability.^{3a,o} More specifically, it was shown that an aromatic substituent decreases their coordination strength because of electron delocalization and steric hindrance. Hence, ligands 3, 4, and 5 seem to follow this trend. Ligand 3, in which the triazoles are substituted by a benzylic group, and ligand 4, for which the triazoles are electronically enriched by the anisyl groups, do bind Zn²⁺. On the contrary, in ligand 5, the triazoles substituted with the electron-deficient nitrophenyl groups are too poor σ donors to coordinate the Zn(II) cation in the absence of guest ligands other than residual water.

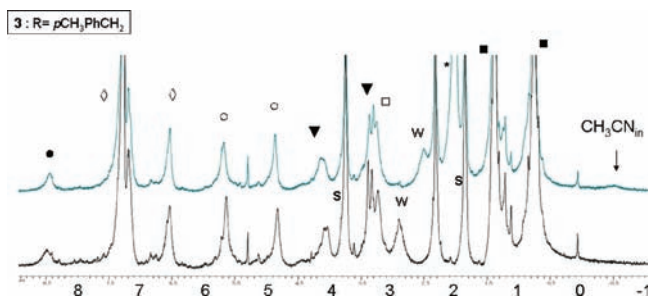


Figure 3. ^1H NMR (CDCl_3 , 250 MHz, 300 K) spectra of Zn(II) complexes based on **3** before (bottom, guest ligand $G = \text{H}_2\text{O}$) and after (top, $G = \text{MeCN}$) the addition of ca. 15 equiv of CH_3CN . (■) $t\text{Bu}$, (□) OCH_3 , (▼) ArCH_2 , (○) OCH_2 , (◇) ArH , (●) H_{tria} . (*, free CH_3CN ; w, residual water; s, residual THF).

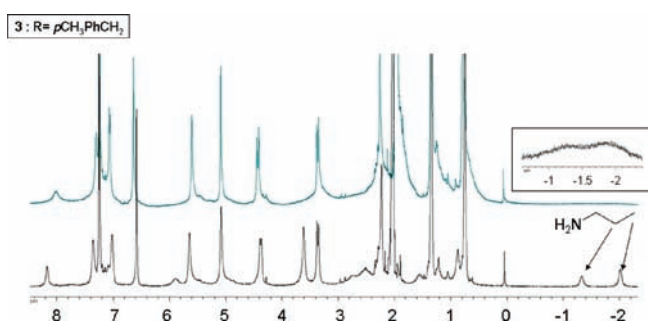


Figure 4. ^1H NMR (CDCl_3 , 500 MHz) spectra of the Zn(II) funnel complex based on ligand **3** ($G = \text{PrNH}_2$) in the presence of ca. 4 equiv of propylamine at 260 K (bottom) and 300 K (top), with the inset showing the low field region.

Coordination of Acetonitrile. Complex $[\text{Zn} \cdot \mathbf{3} \cdot (\text{H}_2\text{O})_n](\text{ClO}_4)_2$ was tested for its ability to coordinate an exogenous acetonitrile molecule. The addition of ca. 15 equiv of CH_3CN into a CDCl_3 solution of complex based on **3** did not drastically modify the spectrum (Figure 3). Nevertheless, a very broad peak at -0.50 ppm indicated partial endocoordination of an acetonitrile molecule to the Zn(II) metal center within the cavity of the calixarene ($G = \text{MeCN}$ in Scheme 2). This interaction is also attested by the upfield shift of the water resonance, showing a competition between acetonitrile and water for the coordination to the metal cation, as previously reported for the **Imme**₃ system.⁸

Coordination of Amines. A better exogenous σ -donor ligand was tested. After the addition of 4 equiv of propylamine into a CDCl_3 solution of $[\text{Zn} \cdot \mathbf{3} \cdot (\text{H}_2\text{O})_n](\text{ClO}_4)_2$, some modifications of the spectrum could be observed at 300 K (Figure 4). The most significant ones are an upfield shift of the H_{tria} peak ($\Delta\delta = -0.29$ ppm), the appearance of two broad resonances in the negative region of the spectrum together with the broadening of the resonances associated with free propylamine. At 260 K, all resonances sharpened, and the presence of one equivalent of propylamine guest deeply included in the calixarene cavity was clearly evidenced with two sharp resonances at $\delta = -1.33$ ppm and $\delta = -2.01$ ppm, integrating for two and three protons versus calixarene, respectively. Hence, like the **Imme**₃-based Zn(II) complexes, a propylamino funnel complex ($G = \text{PrNH}_2$ in Scheme 2) is obtained with, however, a faster in/out exchange process for the amino guest.^{8a} The same experiment carried out with ligand **4** shows a much lower affinity of the metal complex

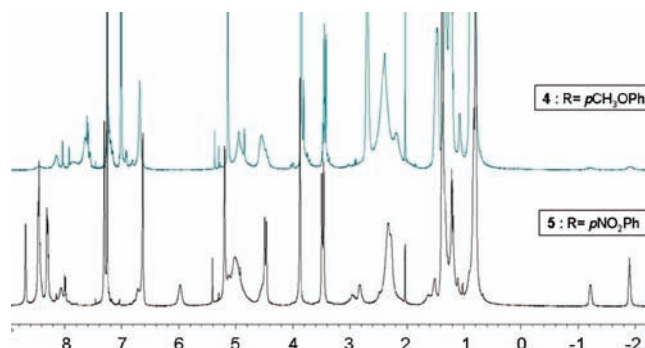


Figure 5. ^1H NMR (CDCl_3 , 500 MHz, 260 K) spectra of the Zn(II) funnel complexes based on ligands **4** (top) and **5** (bottom) in the presence of 4 equiv of propylamine and 3 equiv of heptylamine ($G = \text{PrNH}_2$).

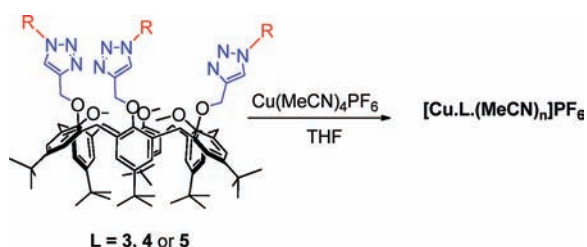
for PrNH_2 . No interaction could be detected at RT (the NMR spectrum remained unchanged), and only partial binding of propylamine was observed at 260 K (see Figure 5, top). Quite surprisingly, whereas ligand **5** does not even form a Zn(II) complex in chloroform, full encapsulation of propylamine was observed at 260 K (see Figure 5, bottom). This shows that the presence of propylamine in solution induces the formation of the Zn(II) complex. Ligand **5** is too electron-deficient to stabilize a Zn(II) dication in the environment provided by the calixarene core when water or acetonitrile are the only extra-donors to complete the coordination sphere (*vide supra*). However, the presence of a good donor like PrNH_2 induces the formation of the host–guest adduct thanks to extra stabilization arising from the encapsulation of the alkylamine: H-bonding to the methoxy substituents at the small rim and $\text{CH} \cdots \pi$ interactions between the alkyl chain and the cavity phenyl rings.^{8,10} Such an observation is interesting because it shows that the more electron deficient ligand **5** is better than ligand **4** at promoting the endocoordination of the guest if the latter is a strong σ donor.

We also tested the coordination of an amine bearing a longer alkyl chain. In both cases (ligands **4** and **5**), no coordination inside the cavity of the calixarene was detected. The addition of excess heptylamine eventually led to the decoordination of the Zn(II) cation in the case of **4**. These funnel complexes thus nicely discriminate propylamine versus heptylamine for their coordination to the metal center *via* the cavity. This is attributable to the $t\text{Bu}$ steric hindrance at the large rim that disfavors the inclusion of a longer alkyl chain inside the cavity.^{12b}

Cu(I) Complexes: Host–Guest Interactions with CO and CH_3CN . We then explored the ability of ligands **3–5** to coordinate a softer metal ion such as Cu(I). The synthesis of the complexes consists of the addition of 1 equiv of $\text{Cu}(\text{CH}_3\text{CN})_4\text{PF}_6$ into a degassed THF solution containing the ligand (Scheme 3). In each case, a precipitate appeared, which was isolated by centrifugation to yield the complex as a tan solid.

The ^1H NMR spectra of complexes $[\text{Cu} \cdot \mathbf{3}]\text{PF}_6$, $[\text{Cu} \cdot \mathbf{4}]\text{PF}_6$, and $[\text{Cu} \cdot \mathbf{5}]\text{PF}_6$ recorded in CDCl_3 are shown in Figure 6. The three complexes display a similar signature, i.e. a spectrum with very broad resonances, as illustrated by the $t\text{Bu}$ peaks at ca. 1 ppm. Only the resonances corresponding to the triazolyl substituent R protons remain sharp. As in the tris(imidazole) case, such behavior is attributable to a dynamic equilibrium involving the coordination to the Cu(I) metal center by only two out of the three nitrogenous arms (Scheme 4).^{9a} As far as ligand **5** is concerned, while it remains insensitive to the presence of Zn(II)

Scheme 3. Synthesis of the Three Copper(I) Complexes
(R = *p*-NO₂Ph, *p*-CH₃OPh, or *p*-CH₃PhCH₂)^a



^a As isolated, n = 0 with ligands 3 and 4, and n = 1 with 5.

in the absence of a strong donor guest ligand, its interaction with the softer Cu(I) cation is clearly evidenced by the NMR profile. In the solid state as well as in solution, all three complexes were revealed to be insensitive to dioxygen, even after weeks, like the related tris(imidazolyl) and tris(pyridyl)-Cu(I) complexes. As compared to those complexes, it appears that the R functionalization of the triazole modulates the interactions with CO or CH₃CN.

Interaction of the Copper Complexes with Carbon Monoxide. After CO was bubbled into chloroform solutions of the complexes, the NMR spectra changed dramatically. The phenomenon was reversible since bubbling argon into the solutions gave back the initial spectra. The new NMR signatures, presenting sharp and well-resolved peaks (Figure 6), attested to the formation of well-defined C_{3v} symmetrical complexes. Hence, CO inhibits the “triazole dance” around the metal center, and its coordination to the Cu(I) cation induces the formation of a four-coordinate species. Indeed, Cu(I) compensates the π-back-bonding to the CO ligand with the coordination to all three triazoles, thus adopting a tetrahedral geometry (Scheme 4). For the structurally similar 4 and 5 ligands, the strongest back-donation is logically observed for the more electron-rich triazole donors: $\nu_{\text{CO}} = 2102 \text{ cm}^{-1}$ for [Cu·4·(CO)]PF₆ (R = *p*-MeOPh) and $\nu_{\text{CO}} = 2108 \text{ cm}^{-1}$ for [Cu·5·(CO)]PF₆ (R = *p*-NO₂Ph). However, with ligand 3, the intermediate CO stretch value ($\nu_{\text{CO}} = 2106 \text{ cm}^{-1}$) suggests that subtle differences in the calixarene conformation (evidenced by the chemical shifts for protons H_{Ar}, OCH₃, ArCH₂, *t*Bu) lead, as in the **Imme**₃ case, to slightly different environments for the CO guest.^{9a}

Interaction with Acetonitrile. One interesting observation in the spectra displayed in Figure 6 is the appearance, upon CO bubbling, of a peak of free acetonitrile solely in the case of complex [Cu·5]PF₆. This peak integrates for ca. 1 equiv of CH₃CN per calixarene that necessarily comes from the copper precursor used for the synthesis of the complex. It shows that one acetonitrile molecule remained coordinated to the Cu(I) cation during the synthetic procedure only with the poorly donating ligand 5. When ca. 10 equiv of CH₃CN were added in a CDCl₃ solution of [Cu·3]PF₆, no significant modification of the ¹H NMR spectrum was observed at room temperature (Figure S5, Supporting Information). However, at 260 K, a new peak arising at −1.13 ppm attests to the coordination of an acetonitrile molecule inside the cavity (Figure S6, Supporting Information). Nevertheless, this peak does not integrate for 1 equiv, and in the positive region of the spectrum, the presence of at least two species is clearly observed. When the same addition of CH₃CN was repeated with [Cu·5]PF₆, the profile of the spectrum at 300 K was modified with the appearance for instance of a resonance at

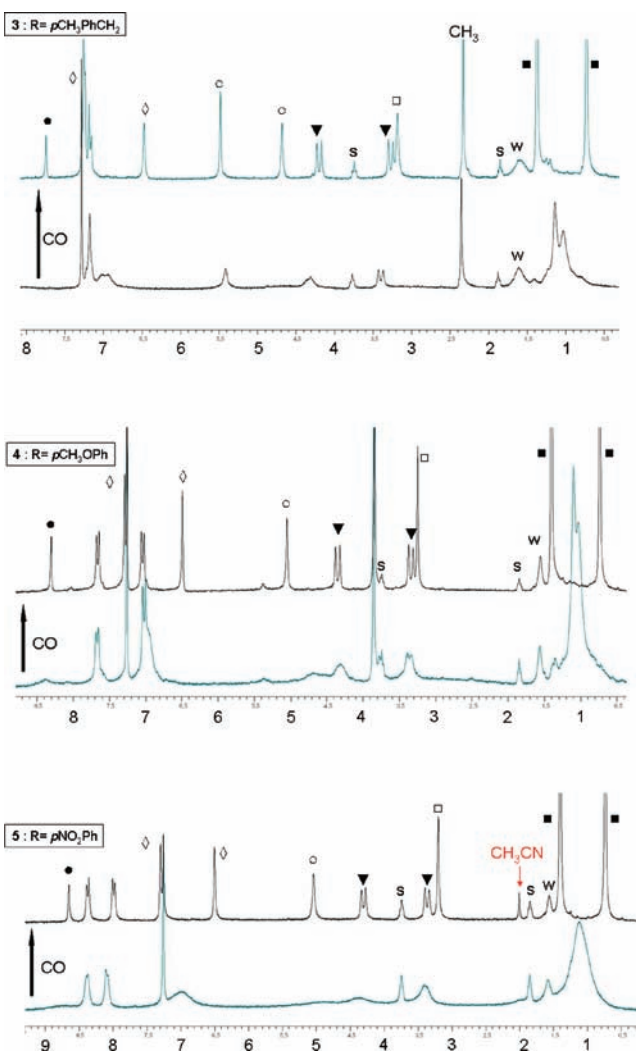


Figure 6. ¹H NMR (CDCl₃, 250 MHz, 300 K) spectra of complexes [Cu·3]PF₆ (top), [Cu·4]PF₆ (middle), and [Cu·5]PF₆ (bottom) before and after the addition of CO. (■) *t*Bu, (□) OCH₃, (▼) ArCH₂, (○) triaCH₂, (◇) ArH, (●) H_{triazole} (w, residual water; s, residual THF).

ca. 8.6 ppm for the H_{triazole} (see Figure S7, Supporting Information). In this case, the addition of an excess of acetonitrile modifies the ligand–copper interaction, thus evidencing the greater affinity of [Cu·5]PF₆ toward nitriles.

Electrochemical Studies. Cyclic voltammetry (CV) studies show that all three tris(triazolyl)Cu(I) complexes behave similarly in CH₂Cl₂/NBu₄PF₆ (see Table 1 and Supporting Information). Under argon, an oxidation peak is observed at $E_{\text{pa}} \approx 0.8 \text{ V}$ versus Fc with subsequent reduction as a broad peak at $E_{\text{pc}} \approx -0.3 \text{ V}$ on the reverse scan. The large difference between cathodic and anodic peak potentials ($\Delta E_{\text{p}} = E_{\text{pa}} - E_{\text{pc}} > 1 \text{ V}$) evidences a high reorganization of the coordination sphere around the copper associated with the change in redox state.¹⁷ Under these solvent conditions, the Cu(I) complexes are stabilized as two or three triazolyl coordinated adducts. Their oxidation leads to the formation of a five-coordinate Cu(II) species (peak $E_{\text{pa}}(\text{a})$ in Figure 7 for [Cu(I)·3]), with coordination of residual water molecules from the solvent: this is fully substantiated by the characterization of the synthesized Cu(II) complex based on ligand 3. Indeed, the corresponding perchlorato dicationic

Scheme 4. “Triazole Dance” around the Cu(I) Center and CO/MeCN Coordination

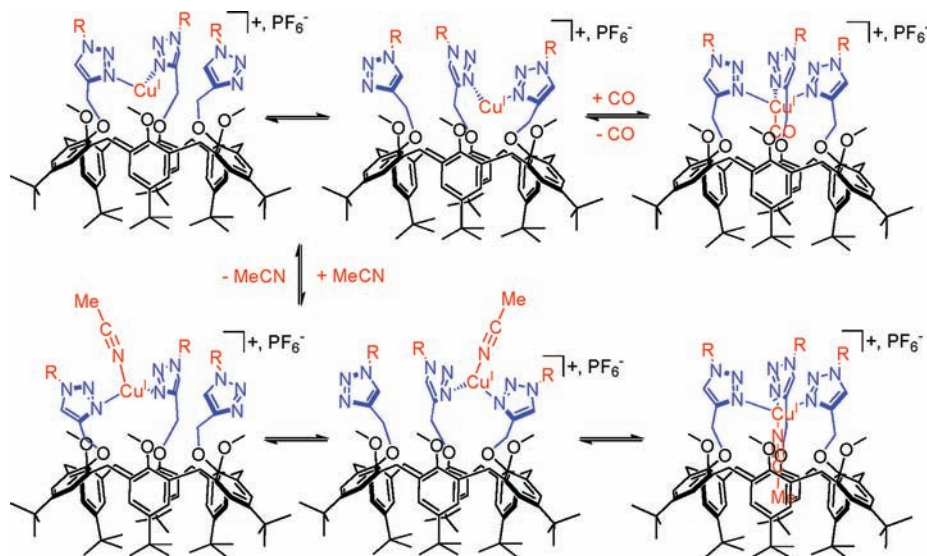


Table 1. Anodic (E_{pa} /V versus Fc) and Cathodic (E_{pc} /V versus Fc) Peak Potential Values from Cyclic Voltammetry at a Vitreous Carbon Electrode of Cu(I) and Cu(II) Complexes Based on Ligands 3–5 and Pic₃ and Imme₃ Ligands in CH₂Cl₂/NBu₄PF₆ 0.1 M (C = 1 mM) under Argon, $\nu = 0.1 \text{ V s}^{-1}$

	CH ₂ Cl ₂	CH ₂ Cl ₂ + CO	CH ₂ Cl ₂ + CH ₃ CN (45 equiv)
[Cu(I)·3]PF ₆	$E_{pa} = 0.77$ $E_{pc} = -0.26$	$E_{pa} = 1.14$ $E_{pc} = -0.25$	$E_{pa} = 0.62$ $E_{pc} = -0.11$
[Cu(I)·4]PF ₆	$E_{pa} = 0.78$ $E_{pc} = -0.37$	$E_{pa} = 1.14$ $E_{pc} = -0.28$	$E_{pa} = 0.56$ $E_{pc} = 0.07$
[Cu(I)·5]PF ₆	$E_{pa} = 0.79$ $E_{pc} = -0.42$	$E_{pa} = 1.19$ $E_{pc} = -0.42$	$E_{pa} = 0.63$ $E_{pc} = 0.02$
[Cu(I)·(Pic ₃)]PF ₆	$E_{pa} = 1.02$ $E_{pc} = -0.35$	$E_{pa} = 1.02$ $E_{pc} = -0.35$	$E_{pa} = 0.76$ $E_{pc} = -0.35$
[Cu(I)·(Imme ₃)]PF ₆	$E_{pa} = 0.52$ $E_{pc} = -0.71$	$E_{pa} = 1.03$ $E_{pc} = -0.71$	$E_{pa} = 0.18$ $E_{pc} = -0.07$
[Cu(II)·3·(H ₂ O) ₂](ClO ₄) ₂	$E_{pc} = -0.35$ $E_{pa} = 0.80$		$E_{pa} = 0.72$ $E_{pc} = -0.17$

complex displays UV–vis and EPR signatures (see Figures S8 and S9, Supporting Information) that are characteristic of a square-based pyramidal environment due to the coordination of all three triazole arms and two extra donors (residual water or CH₃CN depending on the conditions, in endo and exo positions, as shown in the inset of Figure 7 (*vide infra*)).^{9b,c} Such a coordinative environment stabilizes the Cu(II) complexes, which accounts for the much more negative potential (peak E_{pc} (a), Figure 7). This is fully confirmed by the redox behavior in CH₂Cl₂ of the synthesized [Cu(II)·3·(H₂O)₂]²⁺ complex with a reduction peak at $E_{pc} = -0.35 \text{ V}$ (Figure 7 B).

For each Cu(I) complex, the addition of carbon monoxide shifted drastically the oxidation peak (E_{pa} (a) to E_{pa} (b)) toward higher values ($\Delta E_{pa} \approx +400 \text{ mV}$), without significantly affecting the potential value of the reduction peak (E_{pc} (a) $\approx E_{pc}$ (b)) (see Figures 7 and S10–S13, Supporting Information). Such behavior is very similar to that obtained with the Cu(I) complex based on the Imme₃ ligand under the same experimental conditions (i.e., CH₂Cl₂ as a

solvent; see Supporting Information). It highlights the stabilization of the Cu(I) complex through coordination of carbon monoxide, in agreement with the formation of a tetrahedral adduct in which the three triazolyl units are coordinated to the cuprous center. After oxidation (peak E_{pa} (b)), it quickly led back in both cases to the five-coordinated Cu(II) species by water ligation. This behavior confirms the imidazole-like character of the triazole Cu(I) complexes in the presence of CO and contrasts with that observed for the [Cu(I)·(Pic₃)]⁺ complex for which no interaction with CO was detected in voltammetric studies (see Table 1 and Supporting Information).

The effect of acetonitrile on the electrochemical behavior of the Cu complexes was investigated as well. For all triazole-based complexes, the progressive addition of aliquots of CH₃CN into a CH₂Cl₂ solution of the Cu(I) complexes led to a negative shift of the oxidation peak ($\Delta E_{pa} \approx -100$ to -200 mV), together with a positive shift of the reduction peak on the back scan. A particularly important variation of the cathodic peak value was

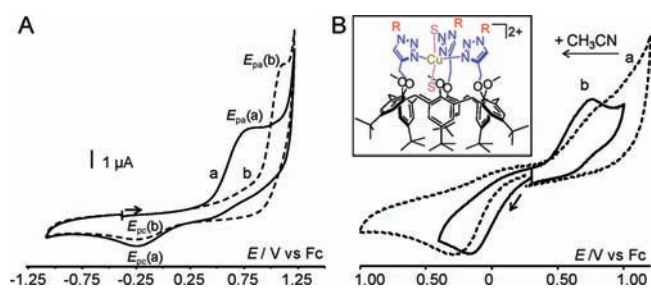


Figure 7. Cyclic voltammograms ($\nu = 0.1 \text{ V s}^{-1}$) at a vitreous carbon electrode in $\text{CH}_2\text{Cl}_2 + \text{NBu}_4\text{PF}_6$ 0.1 M of (A) $[\text{Cu}(\text{I}) \cdot 3]\text{PF}_6$ (1 mM) (a) under Ar (plain line) and (b) under CO (dashed line) and (B) $[\text{Cu}(\text{II}) \cdot 3 \cdot (\text{H}_2\text{O})_2](\text{ClO}_4)_2$ (1 mM) (a) before and (b) after the addition of 150 equiv of CH_3CN . Inset: Schematized five-coordinate $\text{Cu}(\text{II})$ complexes based on tris(triazolyl) ligands.

observed for the $[\text{Cu} \cdot 5]\text{PF}_6$ complex ($\Delta E_{\text{pc}} > 400 \text{ mV}$) compared to its $[\text{Cu} \cdot 3]\text{PF}_6$ and $[\text{Cu} \cdot 4]\text{PF}_6$ analogs (see Figures 8A, B and S14, Supporting Information). All of this denotes an interaction with CH_3CN in fast exchange at the metal center. The high peak separation ($\Delta E_{\text{p}} = E_{\text{pa}} - E_{\text{pc}} > 500 \text{ mV}$ in the three cases) suggests that important rearrangements (conformation, coordination) still operate with the change in redox state, as in pure CH_2Cl_2 , in agreement with the existence of a two, three, or four-coordination in the $\text{Cu}(\text{I})$ state (Scheme 4) and a five-coordination in the $\text{Cu}(\text{II})$ state (Figure 7, inset).

Interestingly, such behavior contrasts markedly with the tris(imidazolyl)-based Cu complex. Indeed, the same experiment performed with complex $[\text{Cu}(\text{I}) \cdot (\text{Imme}_3)]^+$ (progressive addition of CH_3CN into a CH_2Cl_2 solution of the complex, see Figure 8C) led to the appearance of a new reversible system at $\nu = 0.1 \text{ V/s}$ after the addition of 150 equiv of acetonitrile, in agreement with previous electrochemical work in CH_3CN .^{17b} This reversible system is assigned to the transient formation of a $\text{Cu}(\text{I})$ 5-coordinate nitrilo species, which is the thermodynamic species in the $\text{Cu}(\text{II})$ state (similar to that shown in Figure 7, inset). With the triazolyl systems, such a reversible system was never obtained, which can be ascribed to the fact that the $\text{Cu}(\text{I})$ state does not reach the five-coordinate environment. Like for the Pic_3 system (Figure 8D), the much higher oxidation potential (compared to Imme_3) indicates the formation of a four- (or lower) coordinate $\text{Cu}(\text{I})$ species as an intermediate in the $\text{Cu}(\text{I}) \rightarrow \text{Cu}(\text{II})$ redox process. On the other hand, the presence of a single reduction peak after the addition of acetonitrile indicates that the five-coordinate complex is by far the most stable species in the $\text{Cu}(\text{II})$ state with the triazolyl ligands, which is confirmed by the CV of the isolated $\text{Cu}(\text{II})$ species (Figure 7B). This stands in contrast with the redox behavior of $[\text{Cu}(\text{II})\text{Pic}_3]^{2+}$, for which both four- and five-coordinate species were evidenced at this scan rate.¹⁶ Such a difference may be attributable not only to electronic factors (poor donors) but also to the more open access in the exo position for a fifth exogenous ligand with the triazole environment.

DISCUSSION: COMPARISON OF THE TRIS(TRIAZOLE) CORE VERSUS TRIS(IMIDAZOLE) AND TRIS(PYRIDINE)

Zn(II) Coordination. In a noncoordinating solvent, the tris(imidazole)-based $\text{Zn}(\text{II})$ complex is a four-coordinate tetrahedral dicationic species with all imidazolyl arms coordinated to the metal center and one water guest ligand completing the coordination sphere. When the calix[6]arene large rim presents six *t*Bu

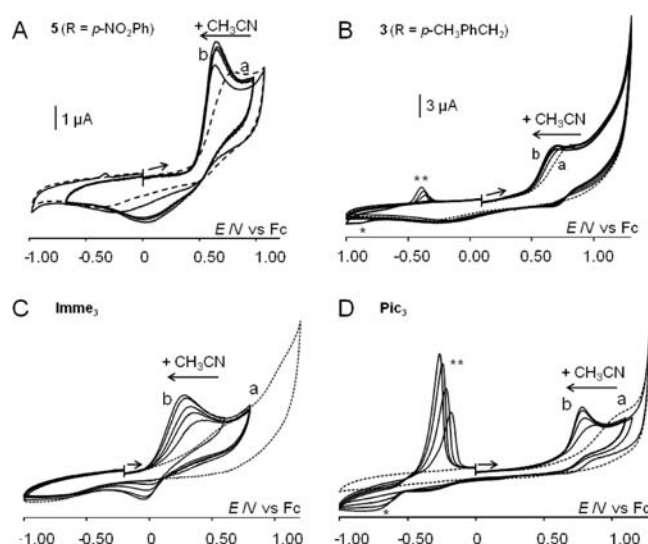
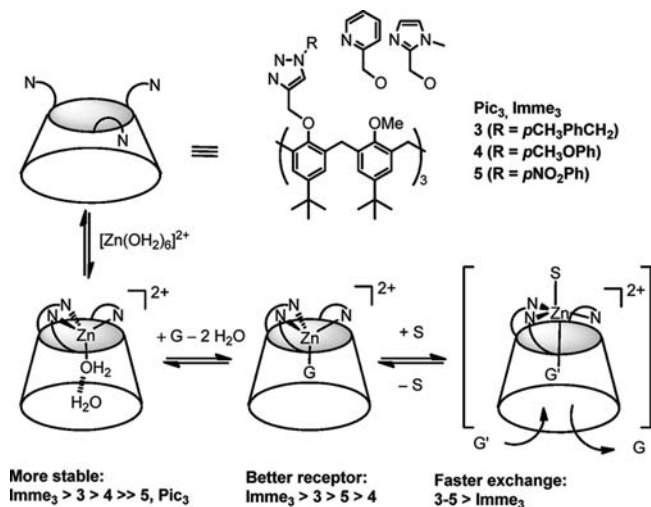


Figure 8. Cyclic voltammograms ($\nu = 0.1 \text{ V s}^{-1}$) at a vitreous carbon electrode in $\text{CH}_2\text{Cl}_2 + \text{NBu}_4\text{PF}_6$ 0.1 M of (A) $[\text{Cu}(\text{I}) \cdot 5]\text{PF}_6$ (1 mM) (a) before (dashed line) and (b) after (plain line) the addition of 150 equiv of CH_3CN [intermediate curves: 15, 45, 75 equiv]; (B) $[\text{Cu}(\text{I}) \cdot 3]\text{PF}_6$ (1 mM) (a) before (dashed line) and (b) after (plain line) the addition of 300 equiv of CH_3CN [intermediate curves: 15, 45, 120, 180, 225 equiv]; (C) $[\text{Cu}(\text{I}) \cdot (\text{Imme}_3)]\text{PF}_6$ (1 mM) (a) before and (b) after the addition of 150 equiv of CH_3CN [intermediate curves: 15, 30, 45, 75 equiv]; (D) $[\text{Cu}(\text{I}) \cdot (\text{Pic}_3)]\text{PF}_6$ (1 mM) (a) before and (b) after the addition of 60 equiv of CH_3CN [intermediate curves: 15, 30, 45 equiv]. (* Cathodic peak corresponding to the $\text{Cu}(\text{I})$ to $\text{Cu}(\text{0})$ reaction. (** Anodic peak corresponding to the $\text{Cu}(\text{0})$ to $\text{Cu}(\text{I})$ reaction.

substituents, the cone cavity is further stabilized by a second water molecule that is strongly hydrogen-bonded to the first one. In strong contrast, with pyridyl arms in place of the imidazoles, no well-defined $\text{Zn}(\text{II})$ complex is formed under the same experimental conditions. This was attributed to the lower donor ability of pyridine versus imidazole. With the triazole derivatives, we have encountered both situations, depending on the nature of the R substituent. On the one hand, with the benzyl group (i.e., 3), a stable $\text{Zn}(\text{II})$ complex is obtained, which displays spectroscopic features almost identical to the imidazole case. In particular, the calixarene conformation, according to the NMR study, looks very similar, which substantiates the formation of an aqua dicationic tetrahedral complex where all three triazole arms coordinate the metal center with the N3 nitrogen of the triazole cycle. On the other hand, when the triazolyl substituent R is a strong electron-withdrawing group ($p\text{NO}_2\text{Ph}$ in 5), no interaction with $\text{Zn}(\text{II})$ is observed in a noncoordinating solvent such as chloroform. The ligand presenting intermediate donor ability (4, $\text{R} = p\text{CH}_3\text{OPh}$) has intermediate behavior leading to the formation of a mixture of different species in fast exchange at room temperature. Obviously, the donor property of the triazole core is tuned by the R substituent, which has a direct impact on the ability of the calixarene-based ligand to stabilize a dicationic Zn complex.

Hosting Properties. The Imme_3 -based $\text{Zn}(\text{II})$ complex is a remarkable receptor for a variety of neutral ligands (provided they can fit in the cavity that allows binding of a single ligand (G) in the endoposition due to geometrical constraints at the small rim). On the NMR time scale, the ligand exchange is a slow process. It is due to two factors: (i) a strong Lewis acidity of the

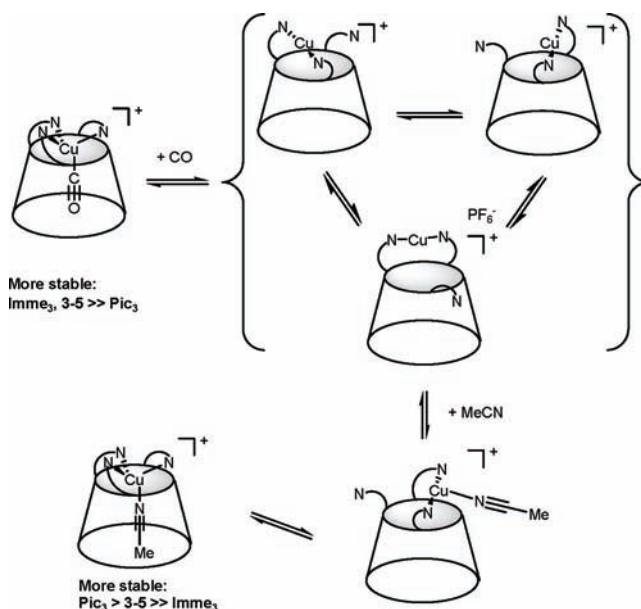
Scheme 5. General Overview of the Coordination and Host–Guest Properties of Calix[6]Arene-Based Tris(Nitrogen) Donors with Zn(II) (*S* = residual water in chloroform; *G* = guest ligand)



dicationic four-coordinate Zn(II) center that precludes a direct dissociative process (that would lead to an unstable three-coordinate intermediate); (ii) steric constraints at the level of the tris(imidazol) core that disfavor binding in the exo position and transient formation of a five-coordinate intermediate allowing guest exchange (as depicted in Scheme 5). Complexes based on the triazole cores revealed lower affinities for organic guest ligands such as amines or nitriles together with a faster exchange process. This may well be attributable to the presence of a nitrogen atom in the α position of the coordinating nitrogen of triazole, instead of a C–H in the imidazole case, which opens the coordination sphere for a fifth ligand. As a result, formation of a five-coordinate complex is favored, and the in–out exchange of the endo ligand is faster. This may also explain why, with ligand **3**, the Zn complex is not as good an endoreceptor as with Imme_3 since a five-coordinate environment must decrease the Lewis acidity of Zn(II). Interestingly also, whereas ligand **5** does not stabilize a Zn complex with water or CH_3CN as a guest ligand, a better donor such as an amine can compensate for the lack of electron density at the triazole site and allow the formation of the corresponding funnel complex with additional stabilizing interactions provided by the calixarene cavity. Quite remarkably, this makes ligand **5** a better receptor for amines in the presence of Zn(II) than **4**, although the latter is more prone to stabilizing Zn(II) Td species with other guest ligands (H_2O , MeCN).

Cu(I) Coordination. The Pic_3 -based Cu(I) complex was actually the first funnel complex to have been characterized by X-ray diffraction. In the presence of a few equivalents of an organonitrile, it forms a highly stable four-coordinate tetrahedral complex with the nitrilo-ligand buried in the calixarene cavity. In strong contrast, the Imme_3 ligand does not give rise to the four-coordinate host–guest adduct in the presence of acetonitrile. With this more electron-donating ligand, only two imidazoles coordinate simultaneously the electron-rich metal center. This gives rise to a dance of Cu(I) between the nitrogenous arms and no guest binding, unless a good π -acceptor such as CO is present (as in Scheme 4). In that case, the third imidazolyl arm undergoes coordination to Cu(I), as the resulting tetrahedral complex is

Scheme 6. General Overview of the Coordination and Host–Guest Properties of Calix[6]Arene-Based Tris(Nitrogen) Donors with Cu(I)



stabilized through π -back-bonding to CO. Of note, the Pic_3 -based Cu(I) complex does not coordinate CO, which is attributable to the lower donor ability of pyridine versus imidazole.

With Cu(I), as depicted in Scheme 6, ligands based on triazole donors display a coordinating behavior that is close to Imme_3 in the absence of any extra donor since Cu(I) undergoes the dance at the tris(triazole) core, and the complexes display poor affinity for nitriles (see NMR results). In addition, all three tris-triazolyl ligands readily give rise to stable four-coordinated species in the presence of CO, very much like for Imme_3 , as shown by spectroscopic (IR, NMR) and electrochemical means. This is in strong contrast to $\text{Pic}_3\text{Cu(I)}$, which displays high affinity for CH_3CN and no coordination of CO. Such a difference can be ascribed to the lower donor effect of the pyridine-based ligand. Electrochemically, the comparative picture is more complicated. In CH_2Cl_2 , the triazole-based systems remain totally irreversible. The oxidation and reduction potentials associated with the three triazole systems lie in between those of Imme_3 and Pic_3 , which fits with intermediate donor properties (see Table 1). In the presence of CH_3CN , their redox behaviors, as observed by CV, resemble more that of Pic_3 with a high potential oxidation peak corresponding rather to a four-coordinate species (or lower) than to a five-coordinate. The redox process however remains fully irreversible (by CV). This may be ascribed to the increased stability of five-coordinate Cu(II) states due to a less sterically hindered environment around the metal center.

CONCLUSION

In this work, we have shown that quite sophisticated ligands associating a coordination sphere and a cavity can be synthesized in two steps with good yields. The herein presented study focused on the coordination and resulting host–guest properties of a tris(triazole) core connected to the hydrophobic cavity of a calix[6]arene. With a strong Lewis acidic cation such as Zn(II), the more electron-rich triazole led to the more stable complexes.

With the softer Cu(I) cation, triazole coordination was less affected by its electron-donating capacities and yielded stable complexes provided, however, the π -acceptor CO ligand was present. Comparison with the analogous tris(pyridyl)- and tris(imidazolyl)-calixarene ligands shows that the tris(triazolyl) cores have mixed coordinating behavior: with Zn(II), depending on the substituent present on the triazole cores, it resembles either the pyridyl (less electron-rich) systems or the imidazolyl (more electron-rich) system. With Cu(I), whatever the substitution pattern is, all triazolyl systems resemble more the imidazolyl complex (CO coordination) except for the redox behavior in the presence of CH₃CN. The study with Zn(II) also highlighted that an important difference between these ligands lies in the different steric hindrance next to the donor atom: the triazole has a nitrogen atom in place of CH for the other two ligands, which decreases the steric hindrance around the metal center and opens more widely a fifth coordination site. Interestingly, this was shown to have an important impact on both the kinetics and the thermodynamics of the systems. Finally, for electronic as well as for steric reasons, the substitution pattern of the triazoles connected at the small rim of the calixarene also changes the host-guest properties of the funnel complexes. This highlights an efficient transmission of information between one edge of the funnel (the coordination core) and the other (the cavity). Hence, the ease of preparation and the versatility of ligands based on 1,4-disubstituted-1,2,3-triazoles whose steric and electronic properties can be tuned at will make them very promising candidates for further applications in coordination chemistry related to biology, catalysis, and materials chemistry.

■ ASSOCIATED CONTENT

S Supporting Information. General procedures, synthesis, and characterization of the ligands and complexes; spectroscopic data; and electrochemical experiments. This material is available free of charge via the Internet at <http://pubs.acs.org>.

■ AUTHOR INFORMATION

Corresponding Author

*E-mail: olivia.reinaud@parisdescartes.fr.

■ ACKNOWLEDGMENT

This research was supported by CNRS and Agence National pour la Recherche [Cavity-zyme(Cu) Project ANR-2010-BLAN-7141].

■ REFERENCES

- (1) (a) Tornøe, C. W.; Christensen, C.; Meldal, M. *J. Org. Chem.* **2002**, *67*, 3057–3062. (b) Rostovtsev, V. V.; Green, L. G.; Fokin, V. V.; Sharpless, K. B. *Angew. Chem., Int. Ed.* **2002**, *41*, 2596–2599.
- (2) (a) Kolb, H. C.; Sharpless, K. B. *Drug Discovery Today* **2003**, *8*, 1128–1136. (b) Tron, G. C.; Pirali, T.; Billington, R. A.; Canonico, P. L.; Sorba, G.; Genazzani, A. A. *Med. Res. Rev.* **2008**, *28*, 278–308.
- (3) (a) Suijkerbuijk, B. M. J. M.; Aerts, B. N. H.; Dijkstra, H. P.; Lutz, M.; Spek, A. L.; van Koten, G.; Klein Gebbink, R. J. M. *Dalton Trans.* **2007**, 1273–1276. (b) Li, Y.; Huffman, J. C.; Flood, A. H. *Chem. Commun.* **2007**, 2692–2694. (c) Mindt, T. L.; Struthers, H.; Brans, L.; Anguelov, T.; Scheinsberg, C.; Maes, V.; Tourwé, D.; Schibli, R. *J. Am. Chem. Soc.* **2006**, *128*, 15096–15097. (d) Happ, B.; Friebe, C.; Winter, A.; Hager, M. D.; Hoogenboom, R.; Schubert, U. S. *Chem. Asian J.* **2009**, *4*, 154–163. (e) Fleischel, O.; Wu, N.; Petitjean, A. *Chem. Commun.* **2010**, *46*, 8454–8456. (f) Ni, X.-L.; Wang, S.; Zeng, X.; Tao, Z.; Yamato, T.

- Org. Lett.* **2011**, DOI: 10.1021/ol102914t. (g) Crowley, J. D.; Gavey, E. L. *Dalton Trans.* **2010**, 39, 4035–4037. (h) Gower, M. L.; Gavey, E. L. *Dalton Trans.* **2010**, 39, 2371–2378. (i) Joly, J. P.; Beley, M.; Selmecki, K.; Wenger, E. *Inorg. Chem. Commun.* **2009**, *12*, 382–384. (j) Maeda, C.; Yamaguchi, S.; Ikeda, C.; Shinokubo, H.; Osuka, A. *Org. Lett.* **2008**, *10*, 549–552. (k) Mullen, K. M.; Gunter, M. J. *J. Org. Chem.* **2008**, *73*, 3336–3350. (l) Ornelas, C.; Aranzaes, J. R.; Salmon, L.; Astruc, D. *Chem.—Eur. J.* **2008**, *14*, 50–64. (m) Fletcher, T.; Bumgarner, B. J.; Engels, N. D.; Skoglund, D. A. *Organometallics* **2008**, *27*, 5430–5433. (n) Meudtner, R. M.; Ostermeier, M.; Goddard, R.; Limberg, C.; Hecht, S. *Chem.—Eur. J.* **2007**, *13*, 9834–9840. (o) Ostermeier, M.; Berlin, M.-A.; Meudtner, R. M.; Demeshko, S.; Meyer, F.; Limberg, C.; Hecht, S. *Chem.—Eur. J.* **2010**, *13*, 10202–10213.

(4) Holm, R. H.; Kennepohl, P.; Solomon, E. I. *Chem. Rev.* **1996**, *96*, 2239–2314.

(5) (a) Malmström, B. G.; Leckner, J. *Curr. Opin. Chem. Biol.* **1998**, *2*, 286–292. (b) Boal, A. K.; Rosenzweig, A. C. *Chem. Rev.* **2009**, *109*, 4760–4779. (c) Kodama, H.; Fujisawa, C. *Metallics* **2009**, *1*, 42–52. (d) Tisato, F.; Marzano, C.; Porchia, M.; Pellei, M.; Santini, C. *Med. Res. Rev.* **2010**, *30*, 708–749. (e) Donnelly, P. S.; Xiao, Z.; Wedd, A. G. *Curr. Opin. Chem. Biol.* **2007**, *11*, 128–133.

(6) Colasson, B.; Save, M.; Milko, P.; Roithová, J.; Schröder, D.; Reinaud, O. *Org. Lett.* **2007**, *9*, 4987–4990.

(7) Colasson, B.; Le Poul, N.; Le Mest, Y.; Reinaud, O. *J. Am. Chem. Soc.* **2010**, *132*, 4393–4398.

(8) With zinc: (a) Sénèque, O.; Rager, M.-N.; Giorgi, M.; Reinaud, O. *J. Am. Chem. Soc.* **2000**, *122*, 6183–6189. (b) Sénèque, O.; Rager, M.-N.; Giorgi, M.; Reinaud, O. *J. Am. Chem. Soc.* **2001**, *123*, 8442–8443. (c) Sénèque, O.; Giorgi, M.; Reinaud, O. *Chem. Commun.* **2001**, 984–985. (d) Sénèque, O.; Rondelez, Y.; Le Clainche, L.; Inisan, C.; Rager, M.-N.; Giorgi, M.; Reinaud, O. *Eur. J. Inorg. Chem.* **2001**, 2597–2604. (e) Sénèque, O.; Giorgi, M.; Reinaud, O. *Supramol. Chem.* **2003**, *15*, 573–580.

(9) With copper: (a) Rondelez, Y.; Sénèque, O.; Rager, M.-N.; Duprat, A.; Reinaud, O. *Chem.—Eur. J.* **2000**, *6*, 4218–4226. (b) Le Clainche, L.; Rager, M.; Reinaud, O. *Inorg. Chem.* **2000**, *39*, 3436–3437. (c) Le Clainche, L.; Rondelez, Y.; Sénèque, O.; Blanchard, S.; Campion, M.; Giorgi, M.; Duprat, A. F.; Le Mest, Y.; Reinaud, O. *C. R. Acad. Sci., Ser. IIC* **2000**, *3*, 811–819.

(10) Coquière, D.; Le Gac, S.; Darbost, U.; Sénèque, O.; Jabin, I.; Reinaud, O. *Org. Biomol. Chem.* **2009**, *7*, 2485–2500.

(11) Rebilly, J.-N.; Reinaud, O. In *Supramolecular Chemistry: from Molecules to Nanomaterials (SMC174)*; Wiley: New York, 2011, in press.

(12) (a) Blanchard, S.; Le Clainche, L.; Rager, M.-N.; Chansou, B.; Tuchagues, J. P.; Duprat, A.; Le Mest, Y.; Reinaud, O. *Angew. Chem., Int. Ed.* **1998**, *37*, 2732–2735. (b) Rondelez, Y.; Rager, M.-N.; Duprat, A.; Reinaud, O. *J. Am. Chem. Soc.* **2002**, *124*, 1334–1340.

(13) Unpublished work.

(14) Ménand, M.; Jabin, I. *Org. Lett.* **2009**, *11*, 673–676.

(15) van Duynhoven, J. P. M.; Janssen, R. G.; Verboom, W.; Franken, S. M.; Casnati, A.; Pochini, A.; Ungaro, R.; de Mendoza, J.; Nieto, P. M.; Prados, P.; Reinhoudt, D. N. *J. Am. Chem. Soc.* **1994**, *116*, 5814–5822.

(16) Sénèque, O.; Campion, M.; Giorgi, M.; Le Mest, Y.; Reinaud, O. *Eur. J. Inorg. Chem.* **2004**, *43*, 1817–1826.

(17) (a) Le Poul, N.; Campion, M.; Izzet, G.; Douziech, B.; Reinaud, O.; Le Mest, Y. *J. Am. Chem. Soc.* **2005**, *127*, 5280–5281. (b) Le Poul, N.; Campion, M.; Douziech, B.; Rondelez, Y.; Le Clainche, L.; Reinaud, O.; Le Mest, Y. *J. Am. Chem. Soc.* **2007**, *129*, 8801–8810.